Unsteady laryngeal airflow simulations of the intra-glottal vortical structures

Mihai Mihaescu[a)]
Department of Aerospace Engineering and Engineering Mechanics, University of Cincinnati, 310 Rhodes Hall, Cincinnati, Ohio 45221-0070

Sid M. Khosla, Shanmugam Murugappan, and Ephraim J. Gutmark[b)]
Department of Otolaryngology-Head and Neck Surgery, University of Cincinnati Medical Center, 231 Albert Sabin Way, Cincinnati, Ohio 4256-0528

(Received 22 October 2008; revised 3 November 2009; accepted 13 November 2009)

The intra-glottal vortical structures developed in a static divergent glottis with continuous flow entering the glottis are characterized. Laryngeal airflow calculations are performed using the Large Eddy Simulation approach. It has been shown that intra-glottal vortices are formed on the divergent wall of the glottis, immediately downstream of the separation point. Even with non-pulsatile flow entering the glottis, the vortices are intermittently shed, producing unsteady flow at the glottal exit. The vortical structures are characterized by significant negative static pressure relative to the ambient pressure. These vortices increase in size and strength as they are convected downstream by the flow due to the entrained air from the supra-glottal region. The negative static pressures associated with the intra-glottal vortical structures suggest that the closing phase during phonation may be accelerated by such vortices. The intra-glottal negative pressures can affect both vocal fold vibration and voice production. © *2010 Acoustical Society of America.* [DOI: 10.1121/1.3271276]

PACS number(s): 43.70.Aj, 43.70.Bk [AL] Pages: 435–444

I. INTRODUCTION

The present research numerically characterizes the unsteady intra-glottal velocity and pressure fields in a three-dimensional, symmetric larynx model of the true vocal folds during the later part of closing. During this phase of phonation, the glottis is divergent. A static model is used here so that the effects of vocal fold movement on the flow are not considered. The primary hypothesis of this work is that intra-glottal vortices form in the superior aspect of the divergent glottis, and that these vortices produce significant negative aerodynamic pressures, relative to both ambient and sub-glottal pressures. These intra-glottal vortices form in a divergent duct due to flow separation and thus will be referred to as flow separation vortices (FSV). The formulated hypothesis is strongly supported by findings in the excised canine larynx model (Khosla *et al.*, 2007, 2008a, 2008b; Murugappan *et al.*, 2009), assuming that the pressures at the glottal exit are similar to the pressures just below the glottal exit, at the same phase. One of the goals of this paper was to test this assumption in a static model since there have been no analytical or computational models that explicitly studied the FSV. In order to test this hypothesis, this study focused on the analysis of the vortical structures developed on the divergent section of the intra-glottal region of the laryngeal airflow, the generation mechanism, and the associated pressures as the vortices travel through and above the glottis.

The hypothesis stated above is clinically important since the findings in the previously mentioned animal models also suggest that these negative pressures play an important role in determining the closing speed of the vocal fold. Gorham-Rowan and Morris (2006) suggested that the vocal fold closing speed is related to the maximum flow declination rate (MFDR). Understanding the mechanisms contributing to the MFDR is clinically important, since the MFDR is highly correlated with vocal intensity (Sundberg and Gauffin, 1979; Holmberg *et al.*, 1988; Gauffin and Sundberg, 1989; Sapienza and Stathopoulos, 1994). Stevens (1998) noted that the rapid reduction in flow is also important for generating acoustic energy over a broad frequency range and showed analytically that increasing the rate of flow shutoff will produce increased energy in the higher harmonics, a theory supported by multiple findings in patients (Klatt and Klatt, 1990; Hanson, 1997; Gobl, 1989).

Fant (1982) showed analytically that a higher MFDR can be obtained by increasing the inertance of the vocal tract, by increasing vocal fold closing speed, or by increasing the maximum lateral vocal fold displacement (MLD). Increasing MLD will increase the elastic recoil forces, which will accelerate vocal fold closing speed and MFDR, and thus augment intensity. However, this mechanism is not consistent with the one study in humans that simultaneously looked at the relationships between intensity and both vocal fold closing speed and MLD. By using image-processing techniques to analyze stroboscopic images in patients under different phonatory conditions, Woo (1996) showed that vocal intensity was highly correlated with maximum vocal fold closing speed but, in contradiction with Fant's theories, not with maximum lateral displacement.

[a)]Author to whom correspondence should be addressed. Electronic mail: mihai.mihaescu@uc.edu
[b)]Also at Department of Aerospace Engineering and Engineering Mechanics, University of Cincinnati, 799 Rhodes Hall, Cincinnati, Ohio 45221-0070.

Woo's (1996) findings are consistent with results in excised canine larynx models (Khosla *et al.*, 2009; Murugappan *et al.*, 2009), which suggest that, under certain conditions, the contribution of the intra-glottal vortices to determining rapid vocal fold closing speed is much higher than the contribution of maximum lateral displacement. Their results also indicate that the FSV are associated with significant intra-glottal negative pressures during closing. It is interesting to note that an earlier study in an excised canine hemilarynx (Alipour and Scherer, 2000) showed negative pressures produced during the later part of closing, when the glottis is divergent. In this case the authors attributed the negative pressures occurring at the upstream glottal sections to Bernoulli effects, flow acceleration, and separation. The negative pressures occurring during closing in the upper portion of the glottis (downstream) were attributed to the curvature of the vocal fold and to rarefaction produced by closing of the folds. These findings in animal models contradict one of the basic assumptions used in many phonatory models: that the pressures downstream of the point of separation are uniform and equal to the ambient pressure (Pelorson *et al.*, 1994; Story and Titze, 1995; Lous *et al.*, 1998). As Krane and Wei (2006) noted, this assumption may not be correct if the glottal flow is significantly unsteady. Therefore, an accurate characterization of the unsteady vortical flow in the intra-glottal region and its interaction with the vocal folds is important.

The use of Computational Fluid Dynamics (CFD) in investigating the non-linear transitional/turbulent glottal airflow has been facilitated by advances in computer technology over the past few decades. Using unsteady CFD solvers, two-dimensional, axisymmetric, and three-dimensional glottal configurations have been analyzed with and without vocal fold motion (Zhao *et al.*, 2001, 2002; Zhang *et al.*, 2002; Hofmans *et al.*, 2003; Alipour and Scherer, 2004; Decker and Thomson, 2007; Mihaescu *et al.*, 2007; Suh and Frankel, 2007). In many of these numerical studies, the sound generated by the laryngeal airflow was considered (Zhao *et al.*, 2001, 2002; Zhang *et al.*, 2002; Mihaescu *et al.*, 2007; Suh and Frankel, 2007). Parametric studies involving the influence of Reynolds number on the flow characteristics and the effect of different divergent glottal angles on the flow separation point have also been performed (Zhang *et al.*, 2002; Alipour and Scherer, 2004; Mihaescu *et al.*, 2007). It is known that for a diverging shape of the vocal folds, when the angle of the glottis exceeds a certain minimal value, the flow separates and vortices are formed immediately downstream of the separation point (Zhao *et al.*, 2001, 2002; Zhang *et al.*, 2002). Although it was recognized that the unsteady vortex shedding results in unsteady forces on the surface of the vocal folds (Zhao *et al.*, 2001, 2002), the features of these vortices have not been investigated in detail. None of these models suggests that the FSV produced significant negative aerodynamic pressures and none of them show the pressures associated with these vortical structures inside the glottis.

There are a few computational larynx models that showed negative wall pressures in the superior aspect of the glottis during closing in addition to the low wall pressures occurring due to Bernoulli effects at the minimum glottal width. However, none of them showed how the pressure field within the glottis changes with the intra-glottal flow evolution. Using Direct Numerical Simulation (DNS), Zhang *et al.* (2002) studied the aeroacoustics of the glottal flow for different phonatory conditions and glottal configurations. During the closing phase, in some of the cases, negative wall pressures and vortices were shown at the superior edge of the glottis exit. These vortices occurred near the glottal exit, therefore having a minimal effect on vocal fold closing speed and MFDR. Zhao *et al.* (2002a) stated that the intra-glottal flow separation vortex "triggers a Kelvin–Helmholtz-type instability of the jet and secondary vortices are formed near the outlet of the glottis."

Using Large Eddy Simulation (LES), Suh and Frankel (2007) showed that the intra-glottal flow attaches to one wall of the divergent duct, which they refer to as the "flow wall." Along that wall, they showed negative intra-glottal pressures in the superior aspect of the glottis. The magnitude of these negative pressures was consistent with the previously mentioned findings in excised canine larynges. However, they described vortices only along the separated flow shear layer, opposite the wall to which the flow was attached. The negative wall pressure was thus related to the adjacent flow rather than to the vortices in the detached shear layer. Therefore, the attached flow described in Suh and Frankel, 2007 does not allow testing of the latter part of our hypothesis—that the flow separation vortices produce significant negative aerodynamic pressures on the wall adjacent to them.

Employing the LES methodology, the present study presents a detailed analysis of the intra-glottal velocity fields, vortical structures, and intra-glottal pressures in a static duct. This analysis will allow us to determine if the flow separation vortices generate significant negative intra-glottal pressures in the superior aspect of the glottis, and thus if the closing phase during phonation may be accelerated by such vortices.

II. METHODS

Computational fluid dynamics methods predict flow characteristics by solving the flow governing Navier–Stokes equations. Within the CFD framework, the steady Reynolds averaged Navier–Stokes (RANS) technique utilizing appropriate two-equation turbulence models (e.g., k-ε or k-ω) cannot accurately describe unsteady flow fields involving flow separation and adverse pressure gradients (Wilcox, 1993). With such models, only information about the local mean flow is computed, and all the flow unsteadiness is filtered out. In flow situations that involve adverse pressure gradients and separation, unsteady RANS based on shear-stress transport k-ω model is superior to other RANS models since it offers a better trade-off between accuracy and efficiency (Suh and Frankel, 2008). In the past few decades, LES has become the major computational tool for studying unsteady turbulent flows (Pope, 2000). LES resolves a large range of turbulent scales (i.e., the energy containing eddies) and thus is able to capture the turbulence dynamics. Only the smallest scales in the turbulent flow need to be approximated by modeling.

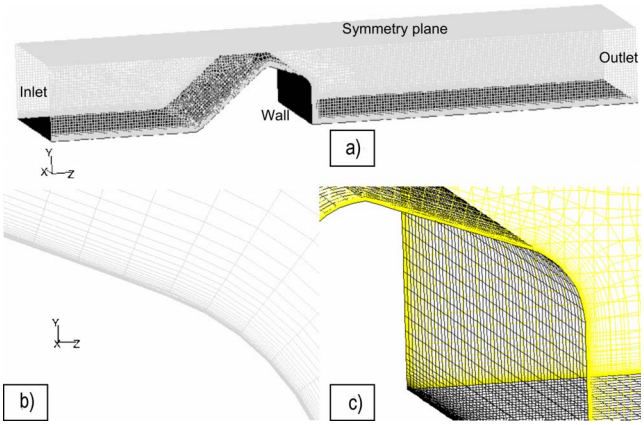

FIG. 1. (Color online) The three-dimensional symmetric larynx model: (a) view of the computational domain showing the inlet and the outlet planes; (b) details of the grid resolution in the y-z mid-plane (mid-coronal plane of the model); the boundary layer region on the 20° divergent side of the glottis is depicted; (c) details of the three-dimensional computational grid in the glottis region.

In the present research, unsteady LES (Fluent Inc.®) is employed to compute the laryngeal airflow through a three-dimensional static and diverging larynx model that assumes symmetry relative to the mid-sagittal plane of the larynx. It is known in both mechanical and computational three-dimensional larynx models that the glottal jet is often asymmetric, attaching to one side or the other of the glottis due to the bistable character of the flow. The phenomenon has been observed and has been analyzed in several studies (Shinwari *et al.*, 2003; Neubauer *et al.*, 2007; Mihaescu *et al.* 2007; Nomura and Funada, 2007; Suh and Frankel, 2007, 2008). On the other hand, experimental studies performed in excised canine larynges using particle imaging velocimetry (Khosla *et al.*, 2008b; Murugappan *et al.*, 2009) showed that flow separation vortices form on both sides of the glottis if the mucosal waves are relatively symmetric. However, if the mucosal waves are significantly asymmetric, the flow does separate on only one side (Khosla *et al.*, 2009). These findings are consistent with results in a self-oscillating physical model with asymmetric vibration reported by Neubauer *et al.* (2007). Since we are interested in the normal situation, where the mucosal waves are relatively symmetric, the present LES study assumes symmetry at the mid-sagittal plane to avoid skewing of the glottal jet relative to the axial direction.

The glottal model is depicted in Fig. 1(a). The vocal folds shape is characterized by a 20° divergent angle corresponding to the closing phase of the phonation cycle. The computational domain consists of a rectangular cross-section of 15.24 mm in the sagittal direction (x), 7.62 mm in the y-direction in the coronal plane (perpendicular to the sagittal plane and parallel to the main flow direction), and 60 mm in the stream-wise direction (z). The minimum distance between the vocal fold and the mid-sagittal plane of the larynx is 1.5 mm resulting in a full glottal width (D_g) of 3 mm. Grid parameters are important for efficient and accurate flow simulation. An unstructured hexahedral body fitted mesh with roughly 7×10^5 computational volumes is used to discretize the computational domain. The Taylor micro-scale (λ_T), which is a measure for the computational cell size, is an important parameter for LES computations. Assuming that the integral length scale (l) is one order of magnitude smaller than the geometrical characteristic length scale defined as the glottal width ($l=0.1D_g$) and a turbulence intensity of 10%, the Taylor micro-scale is (Pope, 2000):

$$\lambda_T=[15\nu_{\text{air}}0.1D_g/(0.1W_{\max})]^{1/2}.$$

Using this definition and considering an air kinematic viscosity of $\nu_{\text{air}}\sim1.79e-5$ m^2/s, a glottal width of $D_g\sim3$ mm, and a maximum axial velocity of $W_{\max}\sim21$ m/s, the Taylor micro-scale is estimated to be $\lambda_T\sim0.2$ mm. Accordingly, the maximum interval size used to discretize the volume of the glottal model is of the same order as the Taylor micro-scale. Detailed LES flow calculations in the near-wall region (i.e., near the vocal folds) are possible due to the high grid resolution used in this region, the computational grid is smoothly stretched in the wall normal direction. Figures 1(b) and 1(c) present details of the computational grid used at the vicinity of the vocal folds. The discretization of the flow governing equations on the computational domain is performed using second order finite-volume schemes. An implicit second order discretization scheme is used for the time integration. The coupling between the velocity field and the pressure field is realized using the semi-implicit method for pressure-linked equation (SIMPLE) algorithm (Van Doormaal and Raithby, 1984). In the present computations, the Smagorinsky–Lilly sub-grid scale model is employed (Lilly, 1966).

The simulations were conducted for a flow rate of 27.5 l/min. The correspondent trans-glottal pressure was approximately 295 Pa (3 cm H_2O). The low flow Mach number (Mach<0.3) allowed using the incompressible flow formulation. A constant axial velocity profile was used as inlet boundary condition (sub-glottal) to match the desired volumetric flux, and 10% turbulence intensity was specified at the inlet surface. The Reynolds number at the minimum glottal width, based on the velocity computed from the bulk flow rate, the glottal width, and the kinematic viscosity of the air was roughly 3500. Symmetry boundary conditions were used at the mid-sagittal plane of the larynx (i.e., upper boundary of the computational domain) and no-slip boundary conditions for velocity were set at the solid surfaces (i.e., side and bottom boundaries of the computational domain). For the outlet plane, a flux conserving zero gradient boundary condition was applied. To reduce the computational time required for the LES unsteady calculations, the flow field was initialized with a previously obtained converged solution based on steady RANS formulation with a k-ε turbulence model.

The time-average flow quantities presented in this study were statistically averaged over a period of 10 000 time-steps (roughly 30 flow-through times), achieving a converged solution at each time-step. The time-step used with the present LES calculations was $\Delta t=0.000\,02$ s. The size of each of the scales developed in the flow field that can be solved by LES is highly dependent on the chosen grid resolution and can be quantified by the energy spectrum. A post-priori spectral analysis was performed in order to check if the grid

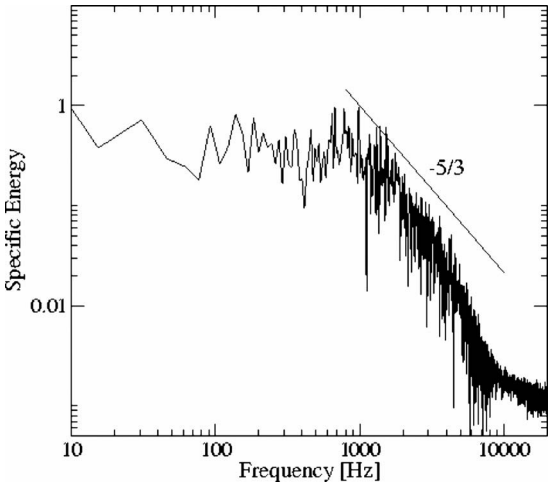

FIG. 2. Turbulent kinetic energy spectrum calculated at a point situated in the supra-glottal region of the larynx. The spectrum follows the −5/3 Kolmogorov power law very well, the spatial resolution of the computational grid being fine enough to resolve a large number of scales within the inertial subrange.

resolution was adequate for solving a large range of scales (i.e., vortical structures) within the inertial subrange (Pope, 2000). The turbulent kinetic energy spectrum in Fig. 2 shows that the energy decay followed the −5/3 Kolmogorov power law, so that the resolution used in the simulations was fine enough to resolve about one order of magnitude of the inertial subrange, a condition required by LES.

III. RESULTS

The time-averaged axial velocity distributions, as predicted by LES, in the mid-coronal plane (y-z mid-plane) of the computational domain are shown in Figs. 3 and 4. The mean flow solution [Figs. 3 and 4(a)] describes the acceleration of the flow due to the convergent geometry of the vocal folds. A maximum velocity was reached at the site of the minimum distance between the glottis and the symmetry plane (i.e., upper boundary of the computational domain). Further downstream, the flow decelerated due to the sudden expansion of the geometry in the lateral direction. The resulting adverse pressure gradient separated the flow from the 20° divergent side of the glottis. A recirculation flow region developed downstream of the separation point that was initiated at the minimum glottal width. Negative axial velocities very close to the wall were associated with this reversed flow region, as shown in Fig. 4(b). The time-averaged axial velocity profiles were extracted along lines situated in the mid-coronal plane of the computational model, at different locations in the flow direction, downstream of the minimum glottal width region as presented in Fig. 4(a). In the intra-glottal region, additional energy that sustains this recirculation bubble was provided by the entrained air from the supra-glottal region.

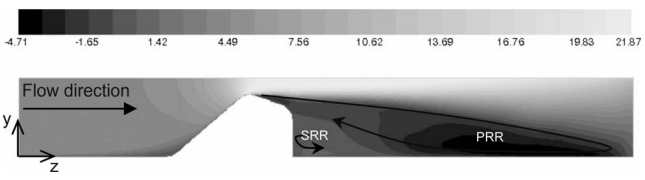

FIG. 3. Time-averaged axial velocity distribution (m/s) as calculated by LES in the mid-coronal plane of the larynx model. Flow separation occurs at the diverging side of the glottis and recirculation regions identified by negative axial velocity values are developed. The maximum velocity occurs at the site of the minimum glottal width (21.87 m/s), while the minimum velocity in the recirculation region is −4.71 m/s. Note: PRR—primary recirculation region; SRR—secondary recirculation region.

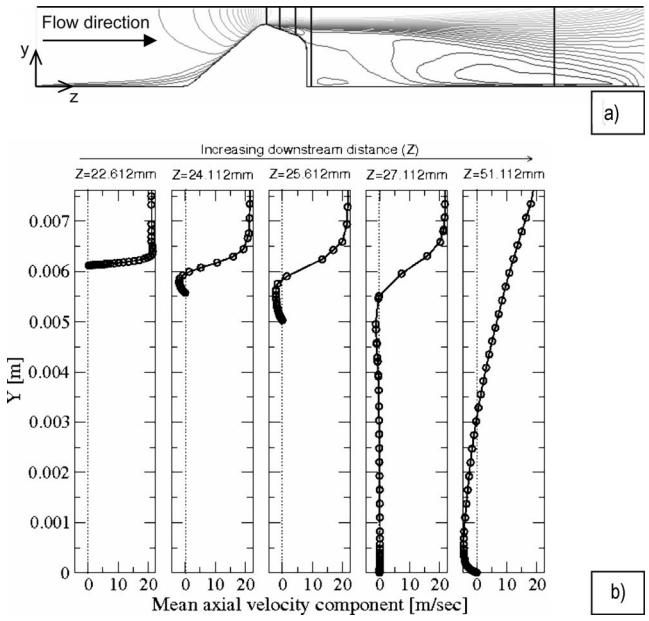

FIG. 4. Time-averaged axial velocity distribution (m/s) as calculated by LES in the mid-coronal plane: (a) location of the lines along which the data was extracted; (b) plots of the time-averaged axial velocity profiles extracted along the lines situated at different locations in the flow direction (z).

The laryngeal airflow was unsteady even with stationary vocal folds. Snapshots of static pressure distributions and velocity vector at different time instances ($t=3.8\times10^{-4}$, $t=5.0\times10^{-4}$, and $t=6.20\times10^{-4}$ s) during the LES calculations are presented in Figs. 5(a)–5(c). These close-ups of the *instantaneous* flow through the glottis at different time stages showed that intra-glottal vortical structures were generated between the divergent slope of the vocal folds and the separated center jet, just downstream of the separation point. The core of these vortical structures was characterized by significant negative static pressure values relative to the surrounding static pressure field. The evolution and convection of these structures resulted in a non-uniform and unsteady static pressure distribution on the vocal folds divergent surface. The convective velocity of these vortices was estimated to be approximately 10 m/s.

The surface static pressure on the glottal wall was affected by the passing of the vortex. Figure 6(a) presents the time history plots of instantaneous static pressure monitored in three different locations (P_1, P_2, and P_3) near the vocal folds surface, along the divergent glottal slope in the mid-coronal plane of the model. Details of the instantaneous isocontours of static pressure spatial distributions at the three time instances ($t=2.0\times10^{-4}$, $t=3.6\times10^{-4}$, and $t=5.0\times10^{-4}$ s) marked on Fig. 6(a), and the location of the three monitoring points (P_1, P_2, and P_3) are depicted in Fig. 6(b). Near the vocal fold, as the vortical structure is moving from

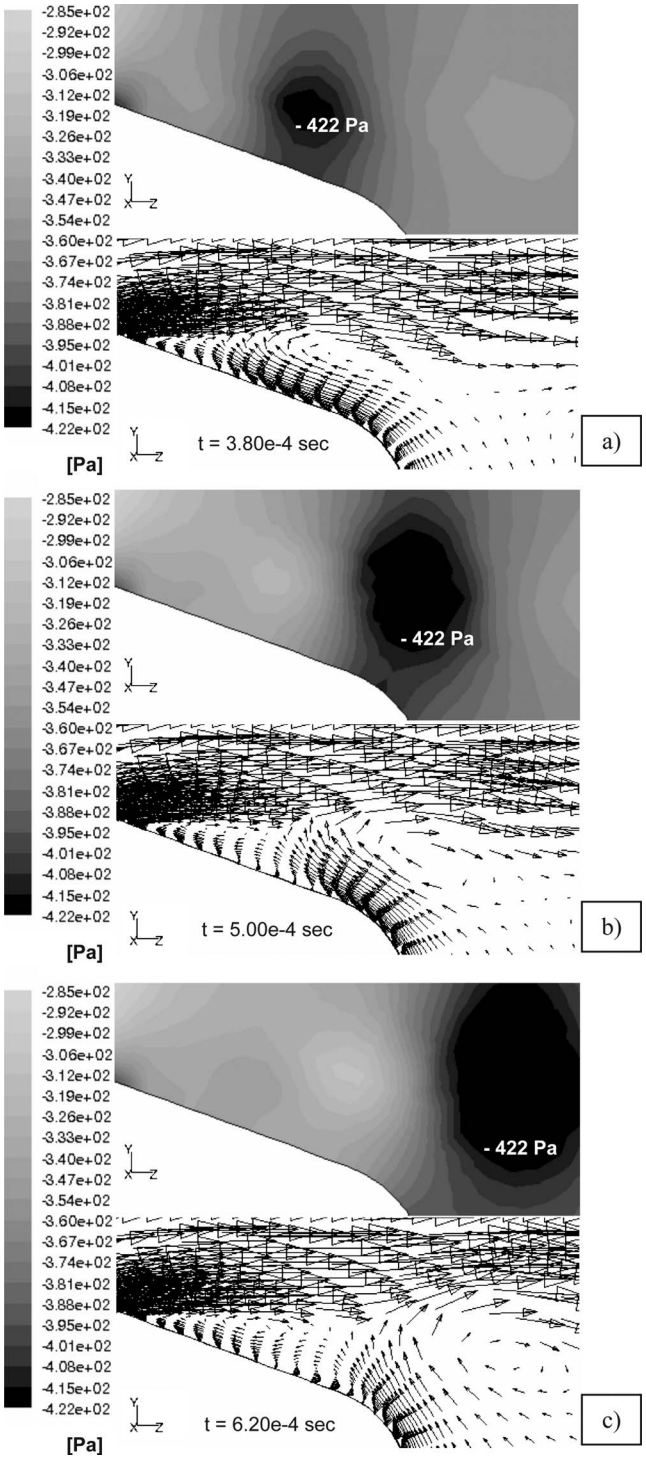

FIG. 5. Flow evolution in the intra-glottal region at three time instances as calculated by LES: (a) 3.8×10^{-4} s, (b) 5.0×10^{-4} s, and (c) 6.2×10^{-4} s. The instantaneous static pressure in Pa (first row) and the corresponding vortical structures represented by velocity vector (second row) are depicted. Note that the legend scale is in Pa: 1 Pa=0.0102 cm H_2O; −422 Pa= −4.30 cm H_2O.

location P_1 to P_3, the static pressure values are decreasing from roughly −320 Pa at P_1 ($t=2.0\times10^{-4}$ s) to −400 Pa at P_3 ($t=5.0\times10^{-4}$ s).

The intra-glottal pressure field was strongly affected by the presence of an intra-glottal vortical structure. Figure 7 presents a comparison in terms of the instantaneous static pressure distributions (pressure drop from sub-glottal pressure) along the centerline of the glottal jet, along a line located in the shear-layer, and along the glottal wall [see Fig. 6(b) for the location of the monitoring lines]. The data are presented for the time instance of $t=3.80\times10^{-4}$ s, when a vortex is formed and is present in the glottis, as shown in Fig. 5(a). As the flow accelerates when it enters the glottis, the pressure decreases. The data extracted along the wall and along the developed shear-layer showed similar profiles, with the pressure values reaching a first minimum at the location of the minimum cross-sectional area (i.e., nearby the glottal entrance) and a second local minimum due to the presence of the intra-glottal vortex. Another observation was that the pressure values on the centerline of the glottal jet have only one minimum that corresponds to the location of the intra-glottal vortex. It should be also noted that the low pressure

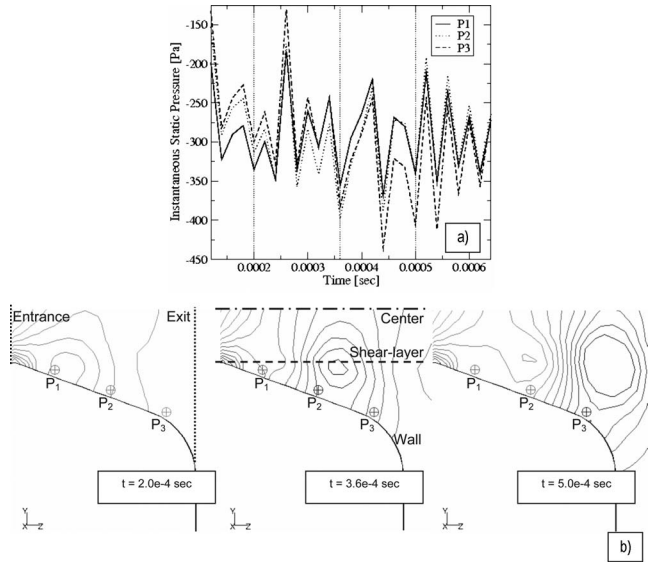

FIG. 6. Intra-glottal static pressure evolution (Pa) in time and space: (a) time history plots of instantaneous static pressure monitored in three different points; (b) locations of the monitoring lines (center, shear-layer, wall) and points (P_1, P_2, and P_3) and the static pressure distributions at three time instances ($t=2.0\times10^{-4}$ s, $t=3.6\times10^{-4}$ s, and $t=5.0\times10^{-4}$ s) indicated in Fig. 6(a).

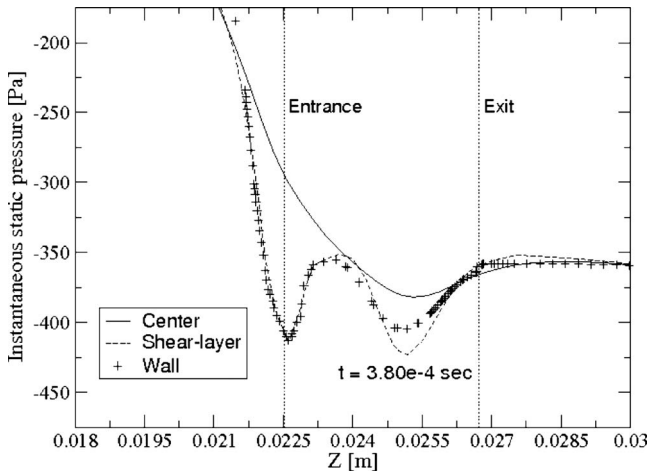

FIG. 7. Instantaneous intra-glottal static pressure distributions (Pa) at the time instance of $t=3.8\times10^{-4}$ s along the centerline of the glottal jet, along a line located in the shear-layer, and along the glottal wall as shown in Fig. 6(b). Note that the glottal entrance and exit are marked on the figure.

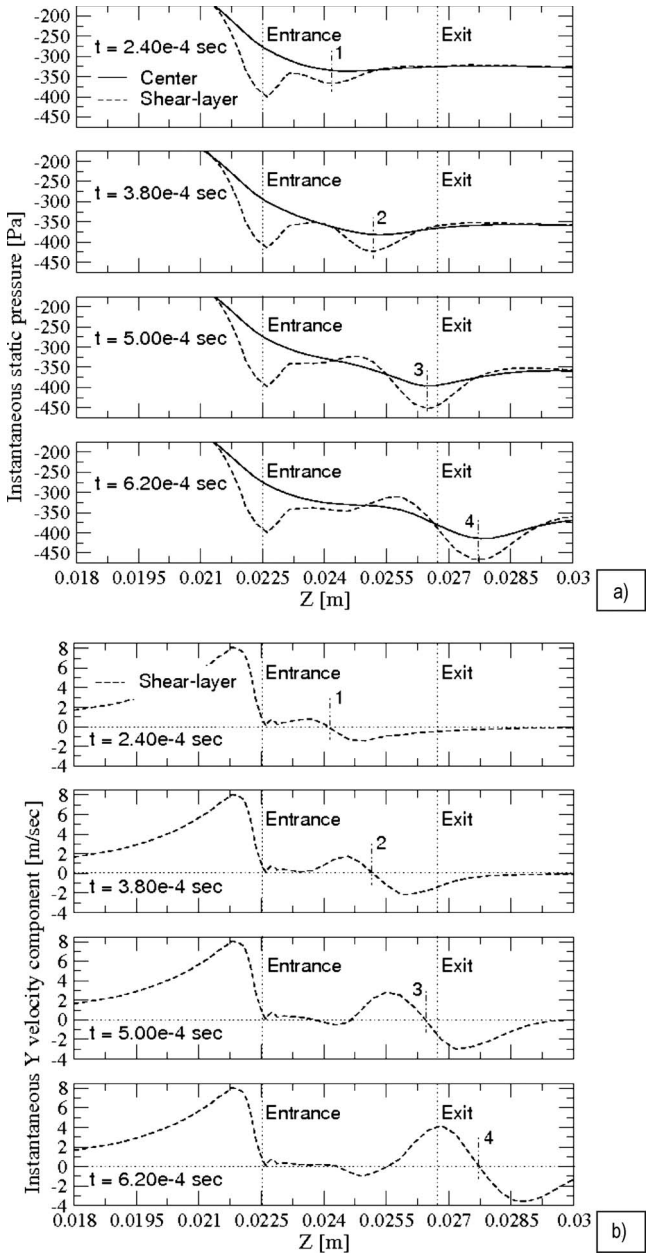

FIG. 8. Time sequences of pressure and Y velocity component profiles associated with intra-glottal vortex evolution: (a) static pressure distributions (Pascal) at four time instances ($t=2.4\times10^{-4}$ s, $t=3.8\times10^{-4}$ s, $t=5.0\times10^{-4}$ s, and $t=6.2\times10^{-4}$ s) along the glottal jet centerline and along the developed shear-layer. (b) Y velocity (m/s) plots at four time instances ($t=2.4\times10^{-4}$ s, $t=3.8\times10^{-4}$ s, $t=5.0\times10^{-4}$ s, and $t=6.2\times10^{-4}$ s) along the developed shear-layer. Note that with 1, 2, 3, and 4 marked on the figure, the locations of the vortex at each of the four time instances are analyzed and Y velocity is the velocity component normal to the flow direction.

values induced by the intra-glottal vortex were lower than the wall pressure values developed at the minimum glottal width.

As the vortex was convected downstream by the flow, it gained strength and increased in size. This resulted in an increase in magnitude of the negative static pressure that characterizes the vortex core. This is presented in Figs. 8(a) and 8(b) using time sequences of static pressure and of Y velocity component plots along the developed shear-layer in the mid-coronal plane (y-z mid-plane). Note that the pressure in Fig. 8(a) is plotted along the glottal jet centerline and the

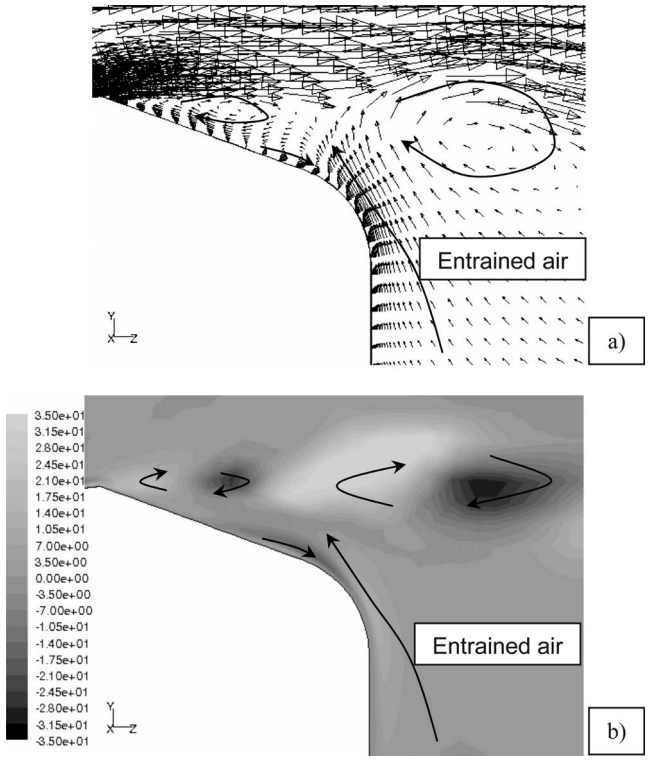

FIG. 9. Instantaneous flow characteristics in the intra-glottal region at the time instance of $t=6.4\times10^{-04}$ s: (a) instantaneous velocity vectors (m/s); (b) the corresponding contours of helicity (m/s^2).

Y velocity is the velocity component in the coronal plane normal to the stream-wise flow direction (z). The four time instances chosen are of $t=2.40\times10^{-4}$, 3.80×10^{-4}, 5.0×10^{-4}, and 6.20×10^{-4} s and relevant data for the last three time successions were presented also in Figs. 5(a)–5(c). While the vortex traveled from position 1 (time instance of $t=2.40\times10^{-4}$ s) to position 4 (time instance of $t=6.20\times10^{-4}$ s), the pressure in the vortex core decreased from roughly −370 to −470 Pa [Fig. 8(a)], whereas the maximum absolute value of the Y velocity component, extracted along the shear-layer that passes through the vortex, increased four times from roughly ±1 to ±4 m/s [Figs. 8(b)].

The strengthening of the intra-glottal vortices as they traveled downstream through the divergent section of the glottis was attributed to the entrained air from the supra-glottal region. This is demonstrated in Fig. 9 that shows a close-up of the instantaneous velocity vectors and the corresponding contours of helicity (m/s^2) at a time instance of $t=6.4\times10^{-4}$ s. Helicity is a scalar quantity defined as the dot product of the velocity and vorticity vectors and it is used as a method to visualize vortical structures since its sign characterizes locally the direction of the swirl with respect to the main flow direction (Degani *et al.*, 1990). A positive sign for helicity means that the rotation is in the same direction as the main flow, and negative means that the rotation is in the opposite direction. The helicity calculated near the glottal wall indicated that there was a strong entrainment of air from the supra-glottal region that interacted with the wall (vorticity generated near by the wall due to the viscous effects) and dominated the near-wall region at the exit of the glottis.

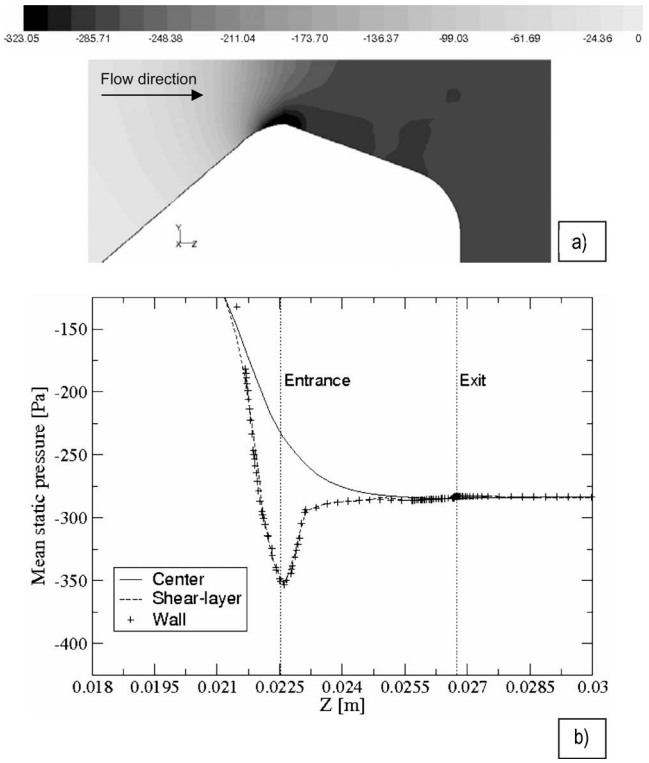

FIG. 10. Time-averaged intra-glottal static pressure distribution (Pa) as calculated by LES in the mid-coronal plane: (a) detail of the static pressure distribution in the mid-coronal plane; (b) comparisons of the mean wall static pressure values with the pressure predicted along the centerline and shear-layer of the glottal jet.

The *time-averaged* static pressure field calculated by LES in the mid-coronal plane of the model is presented in Fig. 10(a). Averaging the pressure data over 10 000 time-steps filtered out the intra-glottal pressure variations due to the presence of the vortices as it was earlier shown in the instantaneous data (Fig. 5). The calculated mean static pressure decreased on the convergent wall of the glottis as the flow accelerated due to glottal channel narrowing [Figs. 10(a) and 10(b)]. The minimum static pressure, on the surface of the vocal folds, was found at the location of minimum cross-sectional glottal area. This was due to the highest flow velocity at the minimal glottal area associated with the effect of the glottis curvature on the pressure field, as explained by Gauffin and Liljencrants (1988). Following the flow direction along the glottal wall, downstream of the minimum cross-sectional area, a slight pressure recovery was found. However, the intra-glottal wall pressure was still lower as compared with the centerline pressure, as shown in Fig. 10(b), in particular, for the region located in the first half of the divergent glottis where the separation induced vortices are produced. The higher pressure found in the center of the intra-glottal flow (higher than the calculated pressure on the wall) is also a condition for the flow to be able to follow the expansion of the divergent glottis (Gauffin and Liljencrants, 1988).

The characteristic frequencies of the intra-glottal and supra-glottal vortical structures were analyzed using velocity spectra. The spectra were obtained by recording the axial velocity time-history at several monitoring points and per-

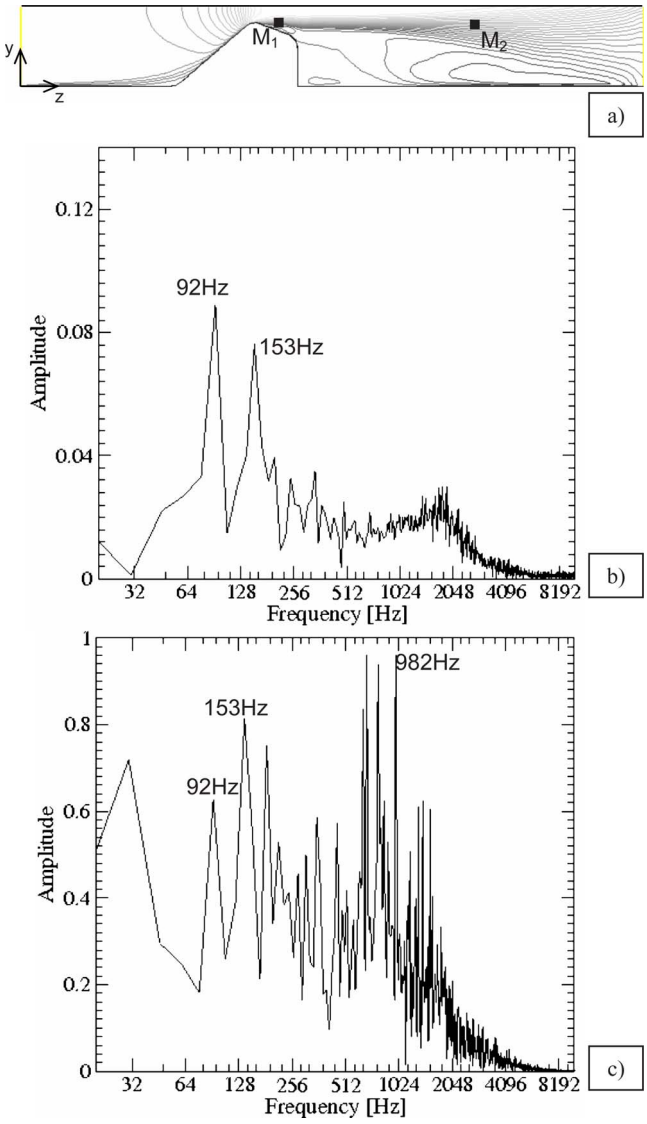

FIG. 11. (Color online) Spectral analysis of the vortical structures: (a) the locations of the monitoring points (M_1 and M_2) in the glottal shear-layer; (b) intra-glottal dominant frequencies at M_1; (c) supra-glottal dominant frequencies *at* M_2.

forming discrete Fourier transforms. Figures 11(b) and 11(c) show the frequency spectra obtained at two locations in the shear layer as marked in Fig. 11(a). The dominant frequencies in the intra-glottal region [Fig. 11(b)] were 92 Hz (St $\sim$0.013) and 153 Hz (St$\sim$0.022), while further downstream, in the supra-glottal region, the dominant frequencies were around 1000 Hz (St$\sim$0.143) [Fig. 11(c)]. The Strouhal number (St=fD_g/W) was based on the minimum glottal width (D_g) and the mean velocity of the glottal jet at this location ($W\sim 21$ m/s). The 92 and 153 Hz frequencies were detected also in the supra-glottal region of the shear-layer, as a result of the convection of the intra-glottal vortices downstream by the laryngeal jet.

IV. DISCUSSION AND CONCLUSIONS

Experimental and unsteady numerical studies performed in the last few decades suggest that vortical structures develop in the laryngeal airflow (Kucinschi *et al.*, 2006; Khosla

et al., 2007; Zhao *et al.*, 2001; Triep *et al.*, 2005; Mihaescu *et al.*, 2007; Neubauer *et al.*, 2007). These structures are formed in the supra-glottal region due to the shear-layer instabilities of the laryngeal jet. Additional vortices are formed in the intra-glottal region during the closing phase of the phonation cycle due to flow separation in the divergent glottal duct (Zhao *et al.*, 2001, 2002; Zhang *et al.*, 2002; Khosla *et al.*, 2007). The fact that the unsteady vortex shedding results in unsteady forces on the surface of the vocal folds is documented (Zhao *et al.*, 2001, 2002; Zhang *et al.*, 2002), but the characteristics of these vortices and their effect on the intra-glottal pressures have not been addressed in detail. This is important since the intra-glottal pressures can affect both vocal fold vibration and voice production.

The present research deals with laryngeal airflow simulations based on LES approach in a symmetric rigid larynx model. The glottis has a divergent shape with an angle of 20°. The LES results captured the flow separation that occurs at the divergent slope of the vocal folds and the intra-glottal vortices that develop immediately downstream of the separation point. These flow structures induced significant negative static pressures relative to both the ambient pressure field and the maximum subglottal pressure. The vortices were also convected by flow, while increasing in strength, near the divergent section of the glottal wall.

Numerical predictions of the *instantaneous* static pressure distribution on the glottal wall as a function of stream-wise distance were previously reported (Zhang *et al.*, 2002). The calculations were performed using DNS of the laryngeal airflow. The motion of the vocal folds in several idealized axisymmetric models of the human vocal tract was studied with or without the presence of the ventricular folds. It was shown that during the closing phase of the phonation cycle (i.e., divergent glottal shape), lower pressures may appear on the divergent slope of the glottis downstream of the expected low at the minimum glottal width. The negative pressures at the inferior aspect were predominantly due to Bernoulli effects, since the glottis is the narrowest at this point. The negative pressures in the wider superior aspect of the glottis were consistent with the hypothesis that the vortices are characterized by negative pressures. However, no correlations were made between these low pressure values and the vortical structures passing near the glottal wall.

The time-averaged intra-glottal pressure distribution predicted by the present LES calculation was shown to be influenced by the low-negative static pressure values induced by the flow structures developed due to the separation of the flow. Thus, in the first half of the divergent wall of the folds, the pressure was lower as compared to its values toward the symmetry plane of the model. The minimum pressure value found on the glottal wall, at the site of the narrowest glottal width, was followed by a slight pressure recovery in the stream-wise direction. LES data concerning the intra-glottal pressure distribution in a rigid convergent-divergent glottal model that considered both left and right vocal folds were recently reported (Suh and Frankel, 2007). It was shown that the glottal jet skews and attaches to one wall, a severe flow separation occurring on the other/opposite wall of the glottis just downstream of the minimum glottal area. The pressure data, on the side where the flow separates, were found to be slightly higher than the pressures on the opposite wall, where flow attaches. As in the present simulations, the minimum pressure was at the location of the narrowest glottal width on the side where separation occurs. Downstream of the separation point, their results indicated a uniform pressure distribution on the vocal fold; the interaction between the glottal jet and the vocal fold wall through eventually generated structures in the shear-layer not being intense due to the severe separation. In the present LES, due to the assumed flow symmetry, the glottal jet skewing is avoided and there is an important interaction between the intra-glottal structures and the divergent wall of the glottis.

The spectral analysis of the flow data revealed that the vortices developed in the intra-glottal region are characterized by lower frequencies ($St \sim 0.02$) as compared with those developed in the supra-glottal region ($St \sim 0.143$). This suggests that the intra-glottal flow structures are induced at lower frequency as compared with the vortices generated in the supra-glottal region in the glottal jet shear-layer. Experimental studies concerning the flow structures generated downstream of divergent larynx models, and their characteristic frequencies, indicated that the Strouhal number of vortex shedding is approximately 0.145 for glottal flows with the Reynolds number of roughly 2000 (Kucinschi *et al.*, 2006; Zhang *et al.*, 2004). This is in good agreement with our findings ($St \sim 0.143$). The same experiments shown that for glottal flows at different Reynolds numbers (roughly range of $1500 < Re < 3300$), the vortex shedding frequency corresponds to a relatively constant value of the Strouhal number. This behavior was not observed for the low Reynolds number cases ($Re < 1500$).

As shown in both experimental and numerical studies, vortical structures affect the voice production through contributions as monopole, dipole, and quadrupole acoustic sources (McGowan, 1988; Barney *et al.*, 1999; Titze, 2000; Zhao *et al.*, 2001; Zhang *et al.*, 2004; Suh and Frankel, 2007). The monopole acoustic source that is associated with fluid displacement due to acceleration of a moving surface was found to dominate the other acoustic sources at very high vocal fold vibration frequencies (Zhao *et al.*, 2002), while the dipole acoustic source generated by the pressure distribution (fluctuating loading) on a surface was found to dominate for convergent-divergent glottal models (Zhao *et al.*, 2001, 2002; Zhang *et al.*, 2004; Suh and Frankel, 2007). The quadrupole acoustic source is generated by turbulence and it was found to be weak when the vocal folds are vibrating or for a convergent-divergent glottal shape. However, it was found to dominate the sound field for straight and converging glottal shaped models in the absence of vocal folds vibration (Zhang *et al.*, 2004). The intra-glottal separation vortices and their correspondent negative pressures may influence all these acoustic sources.

The negative static pressure on the vocal folds walls that is induced by the intra-glottal vortical structures exerts lateral closing force on the divergent section of the glottis. These forces may result in the acceleration of the closing phase of the phonation cycle relative to the opening phase affecting the monopole acoustic source. This asymmetry of

the cycle may have an important implication on voice generation mechanisms. It is known that rapid glottal closing correlates well with voice intensity and loudness (Sundberg and Gauffin, 1979; Woo, 1996; Stevens, 1998).

In summary, the present LES study of a symmetric larynx model with a divergent glottis shows that the pressure loads on the divergent glottal slope are not uniform and unsteady, and are affected by the vortical structures that are convected by the flow near the vocal folds. It is believed that in the case of a pulsatile flow situation or in the case when the vocal folds are moving, the intra-glottal vortices characteristic to the closing phase will be even more important since they are regulated by the flow cycle. Their strength may be also increased for higher trans-glottal pressures or decreased for a less divergent glottal angle. The process by which these separation vortices are generated implies that in order to characterize them, unsteady computational methods that determine the instantaneous flow field must be used, the steady RANS models not being suitable for such calculations.

The results obtained in the present unsteady computational study prove the hypothesis that intra-glottal vortices form in the superior aspect of the divergent glottis and that these vortices generate significant negative aerodynamic pressures, relative to both ambient pressure and maximum sub-glottal pressure.

ACKNOWLEDGMENT

This project was supported by Award No. R01 DC009435 from the National Institute on Deafness and Other Communication Disorders.

Alipour, F., and Scherer, R. C. (**2000**). "Dynamic glottal pressures in an excised hemilarynx model," J. Voice **14**, 443–454.

Alipour, F., and Scherer, R. C. (**2004**). "Flow separation in a computational oscillating vocal fold model," J. Acoust. Soc. Am. **116**, 1710–1719.

Barney, A., Shadle, C. H., and Davies, P. O. A. L. (**1999**). "Fluid flow in a dynamic mechanical model of the vocal folds and tract. I. Measurements and theory," J. Acoust. Soc. Am. **105**, 444–455.

Decker, G. Z., and Thomson, S. L. (**2007**). "Computational simulations of vocal fold vibration: Bernoulli versus Navier-Stokes," J. Voice **21**, 273–284.

Degani, D., Seginer, A., and Levy, Y. (**1990**). "Graphical visualization of vortical flows by means of helicity," AIAA J. **28**, 1347–1352.

Fant, G. (**1982**). "Preliminaries to analysis of the human voice source," Department of Speech, Music, and Hearing, Quarterly Progress and Status Report (KTH), STL-QPSR Report No. 23(4)/1982, http://www.speech.kth.se/prod/publications/files/qpsr/1982/1982_23_4_001-027.pdf (Last viewed 11/2/2009).

Gauffin, J., and Liljencrants, J. (**1988**). "Modeling the air flow in the glottis," Ann. Bull. RILP **22**, 41–52.

Gauffin, J., and Sundberg, J. (**1989**). "Spectral correlates of glottal voice source waveform characteristics," J. Speech Hear. Res. **32**, 556–565.

Gobl, C. (**1989**). "A preliminary study of acoustic voice quality correlates," Department of Speech, Music, and Hearing—Quarterly Progress and Status Report (KTH), STL-QPSR Report No. 30(4)/1989, http://www.speech.kth.se/prod/publications/files/qpsr/1989/1989_30_4_009-022.pdf (Last viewed 11/2/2009).

Gorham-Rowan, M., and Morris, R. (**2006**). "Aerodynamic analysis of male-to-female transgender voice," J. Voice **20**, 251–262.

Hanson, H. M. (**1997**). "Glottal characteristics of female speakers: Acoustic correlates," J. Acoust. Soc. Am. **101**, 466–481.

Hofmans, G. C. J., Groot, G., Ranucci, M., Graziani, G., and Hirschberg, A. (**2003**). "Unsteady flow through in-vitro models of the glottis," J. Acoust. Soc. Am. **113**, 1658–1675.

Holmberg, E., Hillman, R. E., and Perkell, J. S. (**1988**). "Glottal air flow and transglottal pressure measurements for male and female speakers in soft, normal and loud voice," J. Acoust. Soc. Am. **84**, 511–529.

Khosla, S. M., Murugappan, S., and Gutmark, E. J. (**2008b**). "What can vortices tell us about vocal fold vibration and voice production," Curr. Opin. Otolaryngol. Head Neck Surg. **16**, 183–187.

Khosla, S. M., Murugappan, S., Gutmark, E. J., and Scherer, R. C. (**2007**). "Vortical flow field during phonation in an excised canine larynx model," Ann. Otol. Rhinol. Laryngol. **116**, 217–228.

Khosla, S. M., Murugappan, S., Lakhamraju, R., and Gutmark, E. J. (**2008a**). "Using particle image velocimetry to measure anterior-posterior velocity gradients in the excised canine larynx model," Ann. Otol. Rhinol. Laryngol. **117**, 134–144.

Khosla, S. M., Murugappan, S., Paniello, R., Ying, J., and Gutmark, E. J. (**2009**). "Role of vortices in voice production: Normal versus asymmetric tension," Laryngoscope **119**, 216–221.

Klatt, D. H., and Klatt, L. C. (**1990**). "Analysis, synthesis, and perception of voice quality variations among female and male talkers," J. Acoust. Soc. Am. **87**, 820–857.

Krane, M. H., and Wei, T. (**2006**). "Theoretical assessment of unsteady aerodynamic effects in phonation," J. Acoust. Soc. Am. **120**, 1578–1588.

Kucinschi, B. R., Scherer, R. C., DeWitt, K. J., and Ng, T. T. M. (**2006**). "Flow visualization and acoustic consequences of the air moving through a static model of the human larynx," J. Biomech. Eng. **128**, 380–390.

Lilly, D. K. (**1966**). "On the application of the eddy viscosity concept in the inertial subrange of turbulence," NCAR Manuscript No. 123.

Lous, N. J. C., Hofmans, G. C. J., Veldhuis, R. N. J., and Hirschberg, A. (**1998**). "A symmetrical two-mass vocal-fold model coupled to vocal tract and trachea, with application to prosthesis design," Acta. Acust. Acust. **84**, 1135–1150.

McGowan, R. (**1988**). "An aeroacoustic approach to phonation," J. Acoust. Soc. Am. **83**, 696–704.

Mihaescu, M., Gutmark, E. J., Khosla S. M., Scherer, R. C., and Fuchs, L. (**2007**). "Flow and acoustics simulations based on LES and an acoustic analogy; an application to laryngeal airflow," AIAA Paper No. AIAA 2007-919.

Murugappan, S., Khosla, S. M., Casper, K., Oren, L., and Gutmark, E. J. (**2009**). "Flow fields and acoustics in a unilateral scarred vocal fold model," Ann. Otol. Rhinol. Laryngol. **118**, 44–50.

Neubauer, J., Zhang, Z., Miraghaie, R., and Berry, D. A. (**2007**). "Coherent structures of the near field flow in a self-oscillating physical model of the vocal folds," J. Acoust. Soc. Am. **121**, 1102–1118.

Nomura, H., and Funada, T. (**2007**). "Effects of the false vocal folds on sound generation by an unsteady glottal jet through rigid wall model of the larynx," Acoust. Sci. Technol. **28**, 403–412.

Pelorson, X., Hirschberg, A., van Hassel, R. R., Wijnands, A. P. J., and Auregan, Y. (**1994**). "Theoretical and experimental study of quasisteady—Flow separation within the glottis during phonation. Application to a modified two-mass model," J. Acoust. Soc. Am. **96**, 3416–3431.

Pope, S. B. (**2000**). *Turbulent Flows* (Cambridge University Press, Cambridge, England).

Sapienza, C. M., and Stathopoulos, E. T. (**1994**). "Comparison of maximum flow declination rate: Children versus adults," J. Voice **8**, 240–247.

Shinwari, D., Scherer, R. C., DeWitt, K. J., and Afjeh, A. A. (**2003**). "Flow visualization and pressure distributions in a model of the glottis with a symmetric and oblique divergent angle of 10 degrees," J. Acoust. Soc. Am. **113**, 487–497.

Stevens, K. N. (**1998**). *Acoustic Phonetics* (MIT, Cambridge, MA).

Story, B. H., and Titze, I. R. (**1995**). "Voice simulation with a body-cover model of the vocal folds," J. Acoust. Soc. Am. **97**, 1249–1260.

Suh, J., and Frankel, S. H. (**2007**). "Numerical simulation of turbulence transition and sound radiation for flow through a rigid glottal model," J. Acoust. Soc. Am. **121**, 3728–3739.

Suh, J., and Frankel, S. H. (**2008**). "Comparing turbulence models for flow through a rigid glottal model (L)," J. Acoust. Soc. Am. **123**, 1237–1240.

Sundberg, J., and Gauffin, J. (**1979**). in "Waveform and spectrum of the glottal voice source," *Frontiers of Speech Communication Research*, edited by B. Lindholm and S. Ohman (Academic, New York), pp. 301–320.

Titze, I. R. (**2000**). *Principles of Voice Production* (National Center for Voice and Speech, Iowa City, IA).

Triep, M., Brucker, C., and Schroder, W. (**2005**). "High-speed PIV measurements of the flow downstream of a dynamic mechanical model of the human vocal folds," Exp. Fluids **39**, 232–245.

Van Doormaal, J. P., and Raithby, G. D. (**1984**). "Enhancements of the

SIMPLE method for predicting incompressible fluid flows," Numer. Heat Transfer **7**, 147–163.
Wilcox, D. C. (**1993**). *Turbulence modeling for CFD* (DCW Industries, La Canada, CA).
Woo, P. (**1996**). "Quantification of videostrobolaryngoscopic findings-measurements of the normal glottal cycle," Laryngoscope **106**, 1–27.
Zhang, C., Zhao, W., Frankel, S. H., and Mongeau, L. (**2002a**). "Computational aeroacoustics of phonation, Part II: Effects of flow parameters and ventricular folds," J. Acoust. Soc. Am. **112**, 2147–2154.
Zhang, Z., Mongeau, L., Frankel, S. H., Thomson, S., and Park, J. B. (**2004**). "Sound generation by steady flow through glottis-shaped orifices," J. Acoust. Soc. Am. **116**, 1720–1728.
Zhao, W., Frankel, S. H., and Mongeau, L. (**2001**). "Numerical simulations of sound from confined pulsating axisymmetric jets," AIAA J. **39**, 1868–1874.
Zhao, W., Zhang, C., Frankel, S. H., and Mongeau, L. (**2002b**). "Computational aeroacoustics of phonation, Part I: Computational methods and sound generation mechanisms," J. Acoust. Soc. Am. **112**, 2134–2146.